THE JOURNAL OF PHYSICAL CHEMISTRY A

Article

pubs.acs.org/JPCA

Photooxidation of Trimethyl Phosphite in Nitrogen, Oxygen, and *para*-Hydrogen Matrixes at Low Temperatures

N. Ramanathan,[†] K. Sundararajan,*[,†,‡] R. Gopi,[†,‡] and K. Sankaran[†,‡]

[†]Materials Chemistry and Metal Fuel Cycle Group and [‡]Homi Bhabha National Institute, Indira Gandhi Centre for Atomic Research, Kalpakkam-603102, India

Supporting Information

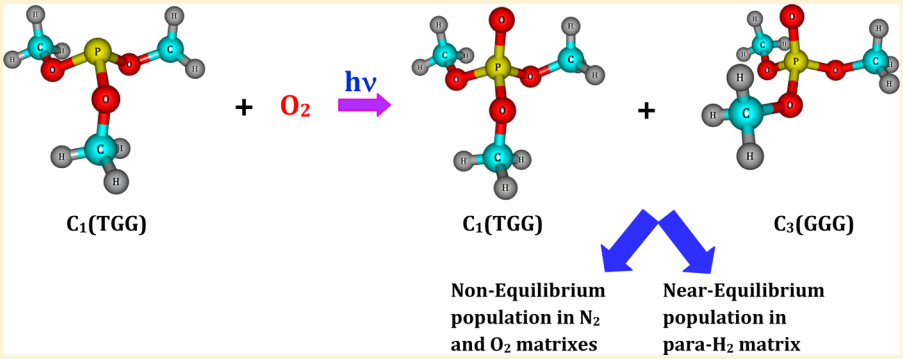

ABSTRACT: Trimethyl phosphite (TMPhite) was photooxidized to trimethyl phosphate (TMP) in N_2, O_2, and *para*-H_2 matrixes at low temperatures to correlate the conformational landscape of these two molecules. The photooxidation produced the trans (TGG)-rich conformer with respect to the ground state gauche (GGG) conformer of TMP in N_2 and O_2 matrixes, which has diverged from the conformational composition of freshly deposited pure TMP in the low-temperature matrixes. The enrichment of the trans conformer in preference to the gauche conformer of TMP during photooxidation is due to the TMPhite precursor, which exists exclusively in the trans conformer. Interestingly, whereas the photooxidized TMP molecule suffers site effects possibly due to the local asymmetry in N_2 and O_2 matrixes, in the *para*-H_2 matrix owing to the quantum crystal nature the site effects were observed to be self-repaired.

1. INTRODUCTION

The study of conformations of molecules with O−P−O and O═P−O connectivity assumes significance because these are the linkages that decide the structures of biologically important phosphate molecules.[1,2] Energy ordering in different conformational isomers is decided by stabilizing electron delocalization (hyperconjugative) and destabilizing steric interactions.[3−6] Although steric interactions keep the bulky groups away from each other, the hyperconjugative delocalization interactions often dictate that the sterically less favorable orientation is an energetically favorable one.[7−12] The conformations of dimethoxy methane (DMM) can be considered to be the classic example in which the sterically crowded gauche conformer turned out to be the ground-state conformer rather than the trans conformer because of the hyperconjugative interaction (the lone pair on oxygen to antibonding σ^*(C−O) delocalization interaction) in the Gauche conformer.[13] Because three or four atoms with a lone pair of electrons are required to observe these interactions, these are pointed out as 1,4 or vicinal (four-centered) interactions. Yet another hyperconjugative interaction, referred to as 1,3 or geminal (three centered) interactions, is normally operative in conformers with two or three atoms with a lone pair of electrons that differ significantly in electronegativity.[14] Phosphorus compounds such as phosphites and phosphates are attractive candidates, where geminal and vicinal hyperconjugation interactions together contribute to their stability. In addition to the electronegativity difference between the phosphorus and oxygen atoms, the presence of a vacant d orbital in the phosphorus atom is a notable contributor to such a geminal interaction. The conformers of alkoxyalkanes (acetals and ketals) and organic carbonates do not earn this extra geminal stabilization because the electronegativity difference between carbon and oxygen is smaller and because of the nonavailability of the vacant d orbital on carbon.[15] Hence, compared to carbon compounds, the compounds of phosphorus are very special because the phosphorus−oxygen linkage enjoys this extra geminal stabilization.

The study of conformations of phosphates is important because tri-*n*-butyl phosphate (TBP) is used as an extractant in the solvent extraction process and TBP is considered to be the workhorse of the nuclear reprocessing industry.[16] The large multitude of conformations for TBP is due to the presence of conformationally flexible butyl groups and its bonding to oxygen. In reprocessing, the metal−TBP complexes are extracted into the

Received: December 7, 2016
Revised: February 24, 2017
Published: February 24, 2017

DOI: 10.1021/acs.jpca.6b12296
J. Phys. Chem. A XXXX, XXX, XXX−XXX

organic phase; consequently, the electron density of the phosphoryl group is substantially reduced. With regard to the conformational orientation of the phosphate, the question arises as to whether metal complexation affects the conformational preferences in phosphates. This question can best be answered by analyzing the conformational energy ordering of phosphites, which lack the phosphoryl group and are considered to be an appropriate representative to model the effect of the phosphoryl group as a result of metal complexation. The simple and straightforward phosphite and phosphate model would then be trimethyl phosphite (TMPhite, $(OCH_3)_3P$) and trimethyl phosphate (TMP, $(OCH_3)_3P{=}O$), respectively. The experimental and computational studies on the conformations of TMPhite have been reported.[17] Through DFT computations, the energy ordering of the different conformers of TMPhite was found to follow the sequence $C_1(TG^{\pm}G^{\pm}$, 0.00 kcal/mol) < $C_s(TG^{+}G^{-}$, 1.22 kcal/mol) < $C_1(TTG^{\pm-}$, 1.38 kcal/mol) < $C_3(G^{\pm}G^{\pm}G^{\pm-}$, 2.46 kcal/mol) (T and G refer to trans and gauche orientations of methyl groups with respect to the phosphorus lone pair, ± represent the clockwise/anticlockwise orientation of methyl groups with respect to the phosphorus lone pair, and C_n refers to the symmetry of the conformer).[18] The dihedral angles of conformers TMPhite and TMP with appropriate reference atoms/groups are given in Table S1 of the Supporting Information. Through effusive (ambient 298 K and high temperature 410 K) and supersonic beam experiments (~100 K), it was confirmed that only the ground state $C_1(TG^{\pm}G^{\pm})$ conformer of TMPhite was populated at 12 K. During deposition at 12 K, the higher-energy $C_s(TG^{+}G^{-})$ and $C_1(TTG^{\pm})$ conformers of TMPhite interconverted and exclusively produced the ground-state $C_1(TG^{\pm}G^{\pm})$ conformer. The barriers for conformer interconversion from higher-energy $C_s(TG^{+}G^{-})$ and $C_1(TTG^{\pm})$ to ground-state $C_1(TG^{\pm}G^{\pm})$ conformer of TMPhite were calculated to be 0.1 and 0.8 kcal/mol, respectively. These small barriers are responsible for higher-energy conformers interconverting to the ground-state conformer of TMPhite during deposition. This process, known as conformational cooling, has been reported well in the literature.[19−21] Because the $C_3(G^{\pm}G^{\pm}G^{\pm})$ conformer is placed at a relatively high energy of ~2.5 kcal/mol with respect to the ground-state conformer, this conformer did not presume any experimental significance. Interestingly, for TMP in the presence of an extra phosphoryl group in comparison to TMPhite, DFT computations disclosed that the conformer with $C_3(G^{\pm}G^{\pm}G^{\pm})$ geometry, the one that is present as the highest-energy conformer in TMPhite, corresponds to the ground state and the ground-state $C_1(TG^{\pm}G^{\pm})$ conformer of TMPhite occurs as the first higher-energy conformer. Unlike TMPhite with the existence of the $C_1(TG^{\pm}G^{\pm})$ conformer experimentally, for TMP, in addition to the ground-state $C_3(G^{\pm}G^{\pm}G^{\pm})$ conformer, the higher-energy $C_1(TG^{\pm}G^{\pm})$ conformer ($\Delta E \approx 0.8$ kcal/mol) has significant population in the low-temperature matrix.[22−24] The barrier at the B3LYP/6-311++G(d,p) level of theory for the interconversion of the higher-energy $C_1(TG^{\pm}G^{\pm})$ conformer to the ground-state $C_3(G^{\pm}G^{\pm}G^{\pm})$ conformer was calculated to be 1.6 kcal/mol.

Reva et al. have reported the photooxidation of trivalent phosphorus (triphenyl phosphine) to pentavalent phosphorus (triphenyl phosphine oxide) at low temperatures.[25] Similarly, phosphite (trivalent phosphorus) can be thought to be photooxidized to phosphate (pentavalent phosphorus) in the presence of oxygen; it will be interesting to perform this experiment to produce TMP in situ from TMPhite under isolated conditions at low temperatures in order to probe the conformational landscape of both molecules. Because the conformational preferences of both the molecules are very different, it will be intriguing to examine whether the intrinsic conformational behavior of TMPhite is conserved as a result of the cage effect of the matrix. If oxidation is achieved in its ground-state $C_1(TG^{\pm}G^{\pm})$ conformer of TMPhite, then an adiabatic transformation to the higher-energy $C_1(TG^{\pm}G^{\pm})$ conformer of TMP will be accomplished. If the matrix, because of its cage effect, preserves this conformer, then the photooxidation of TMPhite can be expected to yield only the higher-energy $C_1(TG^{\pm}G^{\pm})$ conformer of TMP. It will also be interesting to investigate whether any relaxation of the photooxidation product of TMPhite to the ground-state $C_3(G^{\pm}G^{\pm}G^{\pm})$ conformer of TMP occurs in the matrix.

Until recently, the inert (Ne/Ar/Kr/Xe) and diatomic (N_2/O_2) gases were considered only as possible matrixes for matrix isolation experiments. A decade or two ago, *para*-H_2 (*p*-H_2) gas emerged as an alternate and attractive matrix, and it has proved its supremacy compared to conventional inert matrixes.[26−35] Because of the small mass and large-amplitude zero-point vibration, *p*-H_2 is being referred to as a quantum crystal. The quantum crystal nature of solid *p*-H_2 makes it an attractive matrix gas for matrix isolation of guest molecules. The sharp line width in solid *p*-H_2 in comparison to conventional matrixes is one of its exceptional properties. In addition, the *p*-H_2 crystal provides a homogeneous and interaction-free environment for guest molecules embedded in it due to the $J = 0$ rotational wave function, which is completely spherical and symmetric, unlike *ortho*-H_2 (*o*-H_2). The solid *p*-H_2 crystallizes in a pure hexagonal close-packed (hcp) lattice, contrary to other inert and diatomic matrixes, making the optical spectra simple and sharp. The intrinsically restless nature of *p*-H_2 even at absolute zero temperature owing to the large zero-point energy causes multiple trapping sites and crystal defects around the guest molecules to be self-repaired.[28] In addition, the large lattice constant of solid *p*-H_2 causes the interaction to be weaker between the guest and the host molecules, and as a result, the lifetime of the excited states of the guest molecules becomes longer in solid *p*-H_2.[30] The unique properties compared to conventional matrixes make *p*-H_2 a promising matrix for studying the molecular properties at low temperatures, which can mimic the gas-phase behavior. The insignificant or diminished cage effect is also an attractive property for *p*-H_2 for studying the photoproducts including radicals under isolated conditions.[36−39]

The scope of the present study is therefore twofold. The first is to perform the photooxidation of TMPhite at low temperature in O_2-doped N_2 and pure O_2 matrixes to establish a correlation between the conformers of TMPhite and TMP. The second is to accomplish the photooxidation of TMPhite in an O_2-doped *p*-H_2 matrix and compare the results with O_2-doped N_2 in pure O_2 matrixes.

2. EXPERIMENTAL AND COMPUTATIONAL DETAILS

TMPhite (Merck, >98%) and TMP (Merck, >98%) were used without further purification. The samples were, however, subjected to several freeze−pump−thaw cycles before performing the experiments. Nitrogen (Inox, purity 99.9995%) and oxygen (Praxair, purity 99.999%) were used as matrix gases. O_2 was used as a dopant gas for photooxidation experiments. For isotopic scrambling experiments, $^{18}O_2$ (Aldrich; 99 atom %) gas was used. Photoirradiation of the matrix (for about 30 min) was performed using a 1600 W broad band ozone-free high-pressure

DOI: 10.1021/acs.jpca.6b12296
J. Phys. Chem. A XXXX, XXX, XXX−XXX

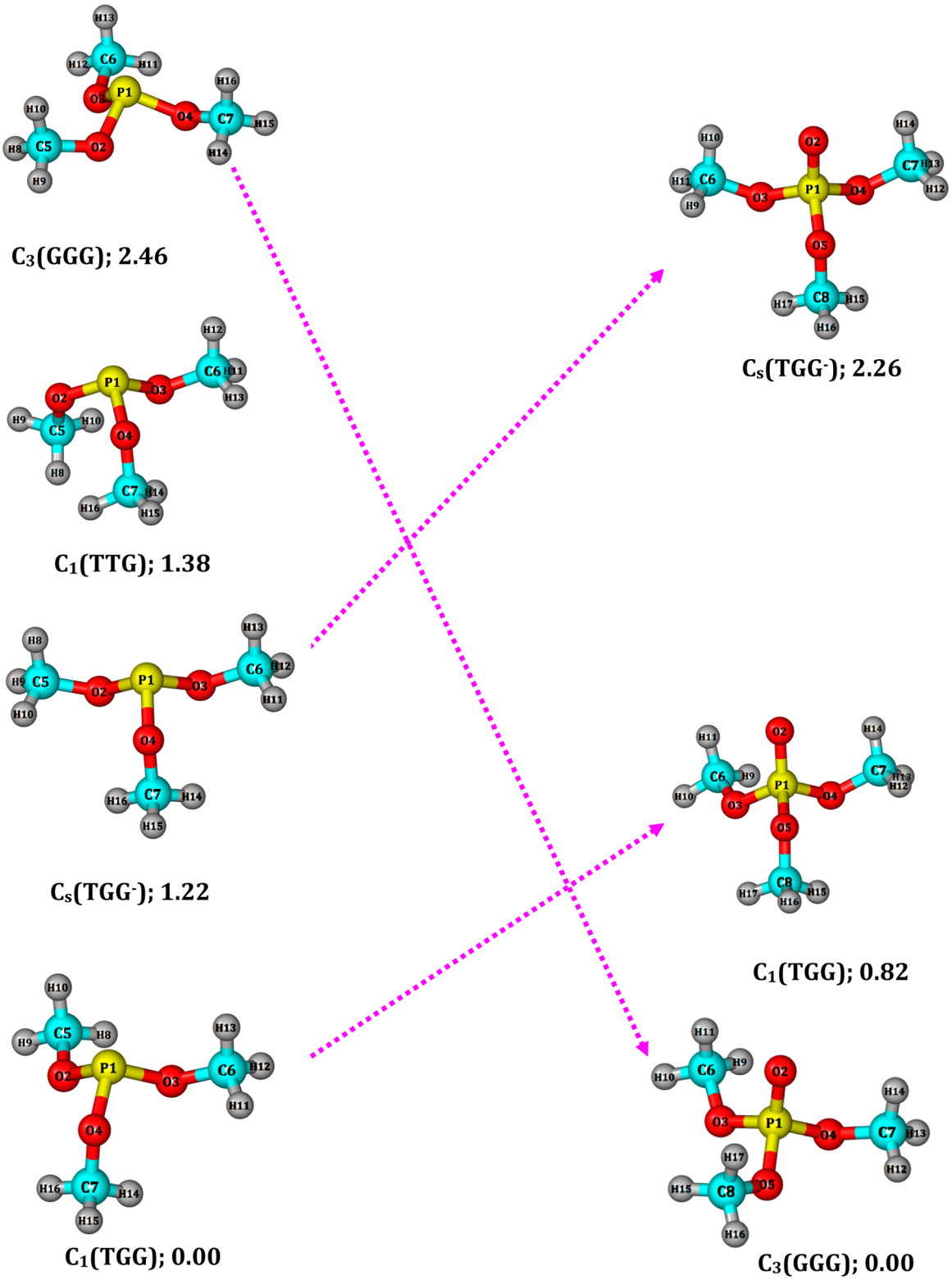

Figure 1. Correlation diagram of the conformations of TMPhite (left) and TMP (right). The ZPE-corrected relative energies in kcal/mol computed at B3LYP level of theory with the 6-311++G(d,p) basis set are shown alongside the conformers.

xenon arc lamp source (model 201-1K air-cooled light source, Sciencetech Inc., Canada). Photoirradiation experiments were carried out on TMPhite by doping 5% O_2 in N_2 and *p*-H_2 matrixes. The photolysis experiment was also conducted on TMPhite in a pure O_2 matrix. TMPhite along with the appropriate gases were mixed in a 1 L stainless steel vacuum chamber and subsequently deposited onto a cold KBr substrate maintained at 12 K. For *p*-H_2, the deposition was accomplished at 2.5 K. The typical concentration of TMPhite to matrix was 1:1000.

The infrared spectra of the matrix-isolated samples were recorded in the range of 5000 to 400 cm^{-1} using a Bruker Vertex

DOI: 10.1021/acs.jpca.6b12296
J. Phys. Chem. A XXXX, XXX, XXX−XXX

Table 1. Relative Energies, Population, and Degeneracies for the Different Conformers of TMPhite and TMP Calculated at the B3LYP and CCSD Levels of Theory with the 6-311++G(d,p) Basis Set

		B3LYP/6-311++G(d,p)[a]		CCSD/6-311++G(d,p)[b]	
conformers	degeneracy	relative energy (kcal/mol)	population (%)	relative energy (kcal/mol)	population (%)
		TMPhite			
$C_1(TG^{\pm}G^{\pm})$	6	0.00	85.7	0.00	88.7
$C_s(TG^{+}G^{-})$	3	1.22	5.5	1.71	2.5
$C_1(TTG^{\pm})$	6	1.38	8.4	1.37	8.7
$C_3(G^{\pm}G^{\pm}G^{\pm})$	2	2.46	0.4	3.29	0.1
		TMP			
$C_3(G^{\pm}G^{\pm}G^{\pm})$	3	0.00	56.5	0.00	41.2
$C_1(TG^{\pm}G^{\pm})$	6	0.82	41.6	0.45	57.8
$C_s(TG^{+}G^{-})$	3	2.26	1.88	2.47	1.0

[a]Corrected for zero-point energy. [b]Single-point energy. (The optimized structure at the B3LYP level of theory was used.)

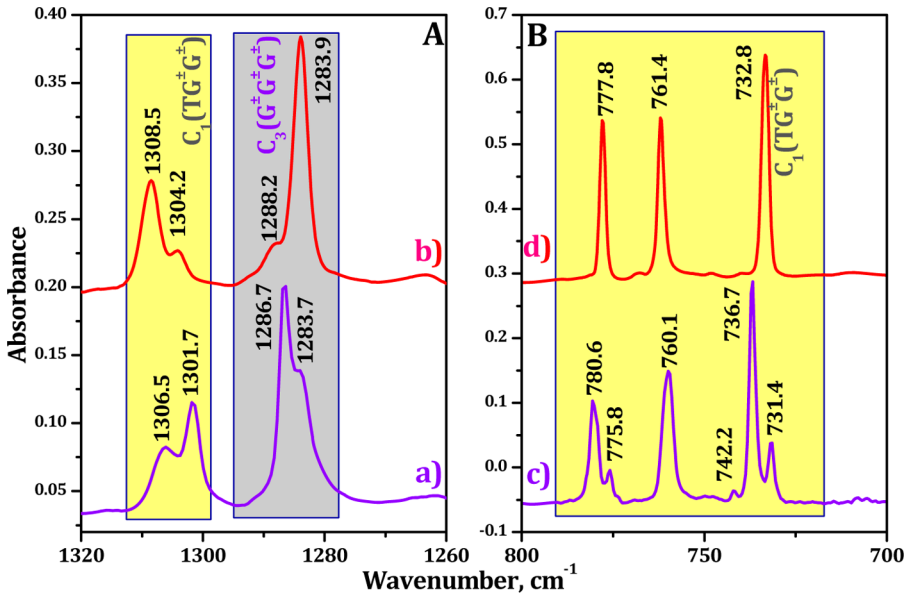

Figure 2. Infrared spectra of matrix-isolated TMP (grid A: P═O stretching region) and TMPhite (grid B: P−O stretching region) in N_2 and p-H_2 matrixes. Grid A: (a) TMP/N_2 at 12 K and (b) TMP/p-H_2 at 2.5 K. Grid B: (a) TMPhite/N_2 at 12 K and (b) TMPhite/p-H_2 at 2.5 K. The typical concentration of TMPhite or TMP to the matrix is 1:1000.

70 FTIR spectrometer with a resolution of 0.5 cm^{-1} using a liquid-N_2-cooled mercury cadmium telluride (MCT) detector. Before and after photoirradiation, the infrared spectra were recorded at 12 K (N_2 and O_2 matrixes) and 2.5 K (p-H_2 matrix). Subsequently, the matrix was warmed to ∼30 K for N_2 and O_2 matrixes and to 4.5 K for p-H_2, kept at this temperature for 15 min, and recooled to ∼12 K (N_2 and O_2 matrixes) and 2.5 K (p-H_2 matrix). The spectra of the matrix after annealing were again recorded.

p-H_2 gas was produced by passing n-H_2 through the ortho/para converter at low temperatures. The details of the experimental setup and the preparation of pure p-H_2 gas are described elsewhere.[40]

DFT computations were used for the optimization of the conformers of TMPhite and TMP. Geometry optimization was performed using a B3LYP hybrid-exchange correlation functional using the 6-311++G(d,p) basis set. Single-point calculations were performed using the CCSD level of theory with the aforementioned basis set. All computations were carried out using a *Gaussian 09* package.[41]

3. RESULTS AND DISCUSSION

A correlation diagram indicating the conformational isomers of TMPhite and TMP together with their ZPE-corrected relative energies is shown in Figure 1. The computed relative energies together with the room-temperature population of the different conformers of TMPhite and TMP and their degeneracies are presented in Table 1. Figure 2 (grid A) shows the infrared spectral features in the P═O stretching region of TMP in N_2 and p-H_2 matrixes. Among the P═O, P−O, and O−C vibrational spectral regions, the P═O stretching region of TMP shows the maximum vibrational wavenumber separation of the two conformers, and hence this region alone is presented in Figure 2. The vibrational wavenumbers that occur at 1286.7/1283.7 and 1306.5/1301.7 cm^{-1} in N_2 and at 1288.2/1283.9 and 1308.5/1304.2 cm^{-1} in p-H_2 matrixes correspond to ground-state $C_3(G^{\pm}G^{\pm}G^{\pm})$ and higher-energy $C_1(TG^{\pm}G^{\pm})$ conformers, respectively.[22,23,40] Because TMPhite does not possess any characteristic phosphoryl group, the P−O and O−C stretching regions are used to obtain its conformational signature. Figure 2, grid B, shows the P−O spectral region of TMPhite. It can be reiterated that through systematic effusive and supersonic beam experiments the ground-state $C_1(TG^{\pm}G^{\pm})$ conformer was alone

DOI: 10.1021/acs.jpca.6b12296
J. Phys. Chem. A XXXX, XXX, XXX−XXX

Table 2. Comparison of Computed Vibrational Wavenumbers of the $C_1(TG^{\pm}G^{\pm})$ Conformer of TMPhite, $C_3(G^{\pm}G^{\pm}G^{\pm})$ and $C_1(TG^{\pm}G^{\pm})$ Conformers of TMP with Experimental Wavenumbers in N_2, O_2, and *p*-H_2 Matrixes[a]

conformers	computed vibrational wavenumber (cm^{-1})[b]	experimental vibrational wavenumber (cm^{-1})			mode assignments
		N_2 matrix	O_2 matrix	*p*-H_2 matrix	
		TMPhite			
$C_1(TG^{\pm}G^{\pm})$	687.8 (186)	731.4, 736.7, 742.2	733.3, 733.8	732.8	P−O stretching
	730.3 (155)	760.1	751.7, 759.9, 763.8	761.4	
	745.7 (67)	775.8, 780.6	775.4, 787.9	777.8	
	1030.8 (333)	1022.2, 1025.1	1019.0, 1025.4, 1029.3	1025.3, 1031.2	O−C stretching
	1047.2 (310)	1030.8, 1035.0	1036.9	1038.9	
	1076.5 (89)	1066.8	1068.4	1070.3	
		TMP			
$C_3(G^{\pm}G^{\pm}G^{\pm})$	1261.2 (213)	1286.7		1285.2[d]	P=^{16}O stretching
	1225.7 (187)	1248.0 (−38.7)[c]		1247.1(−38.1)[c,d]	P=^{18}Ostretching
$C_1(TG^{\pm}G^{\pm})$	1290.1 (265)	1301.7, 1306.5		1309.7[d]	P=^{16}O stretching
	1251.6 (271)	1262.8 (−38.9)[c], 1267.2 (−39.3)[c]		1273.2 (−36.5)[c,d]	P=^{18}O stretching

[a]The computations have been performed at the B3LYP level of theory with the 6-311++G(d,p) basis set. [b]Intensities in km mol^{-1} are given in parentheses [c]The experimental shift of the P=^{18}O stretch with respect to the P=^{16}O stretch is given in parentheses [d]Wavenumbers for TMP in 5% O_2 doped in the *p*-H_2 matrix.

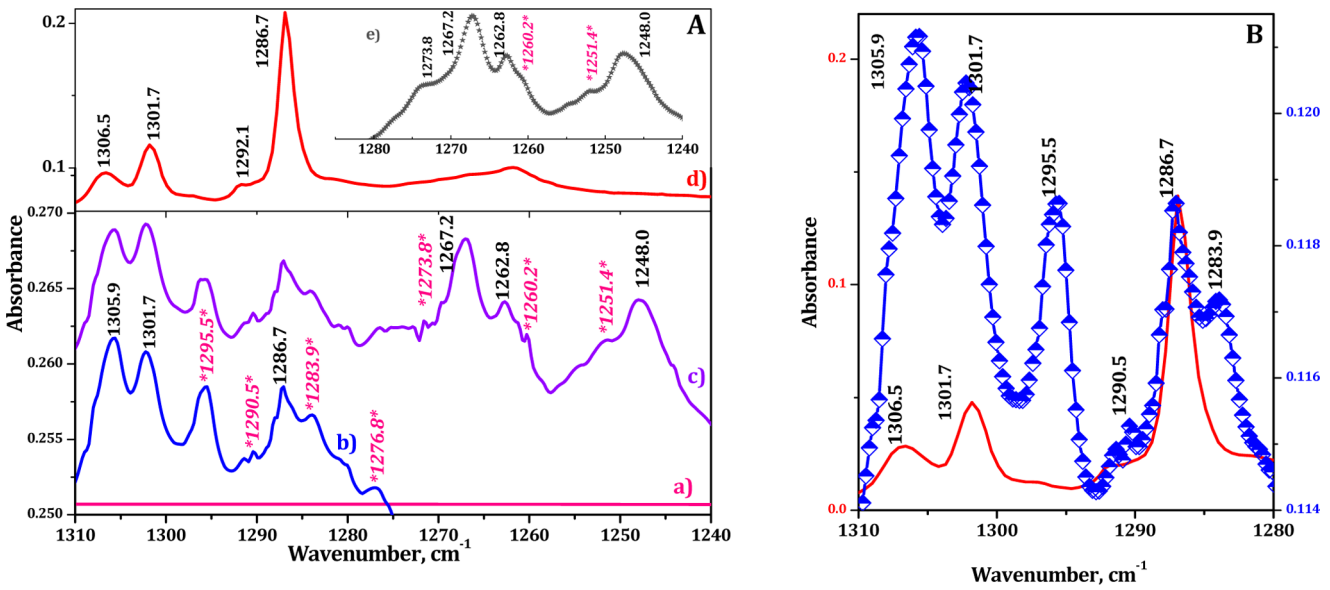

Figure 3. Infrared spectra of oxygen-doped TMPhite in the N_2 matrix (grid A) and conformational yield comparison (grid B) at 12 K in the P=O spectral region of TMP. Grid A: (a) TMPhite/N_2 with 5% $^{16}O_2$ before photolysis at 12 K. (b) Same as in a but photolyzed for 30 min. (c) TMPhite/N_2 with 2.5% $^{16}O_2$ and 2.5% $^{18}O_2$ after photolysis at 12 K. (d) TMP/N_2 with 5% $^{16}O_2$ at 12 K. (e) TMPhite/N_2 with 5% $^{18}O_2$ after photolysis at 12 K (inset). The wavenumbers marked in black correspond to the spectral features that exactly match with pure TMP. The wavenumbers marked in pink are due to the additional features that are produced as a result of the effect of photolysis. Grid B: Blue-[line + symbol], infrared spectra of TMP produced through the photooxidation of TMPhite in the N_2 matrix; red-[line], pure TMP/N_2 with 5% $^{16}O_2$ at 12 K. The typical concentration of TMPhite or TMP to the matrix is 1:1000.

identified, and all of the spectral features observed in the low-temperature matrix correspond to this conformer. NBO analysis revealed that the presence of the phosphoryl group in TMP induces a geminal hyperconjugation interaction and causes the $C_3(G^{\pm}G^{\pm}G^{\pm})$ conformer to be energetically more favorable compared to the $C_1(TG^{\pm}G^{\pm})$ conformer.[17] Because of the absence of the phosphoryl group in TMPhite, the contribution to stability through geminal interaction is appreciably reduced in the $C_3(G^{\pm}G^{\pm}G^{\pm})$ conformer; consequently, this conformer is placed highest in the energy ladder. The computed vibrational wavenumbers of the conformers of TMPhite and the experimental wavenumbers are presented in Table 2.

3.1. Photooxidation of TMPhite in N_2 and O_2 Matrixes.

TMPhite was deposited in N_2 matrix together with O_2 dopant and photolyzed using a broad-band xenon source in an attempt to oxidize TMPhite. Trace a in Figure 3 (grid A) shows the infrared spectrum of matrix-isolated TMPhite with 5% $^{16}O_2$ in an N_2 matrix at 12 K prior to photoirradiation, and trace b presents the spectrum recorded after the photolysis of the above mixture for 30 min. Trace c is the infrared spectrum corresponding to photoirradiation experiments where O_2 is isotopically scrambled with 2.5% $^{16}O_2$ and 2.5% $^{18}O_2$. Trace d is the infrared spectrum of matrix-isolated pure TMP in an N_2 matrix with 5% O_2. The features observed at 1286.7 and 1301.7/1306.5 cm^{-1} in trace d are due to the P=O stretch in the $C_3(G^{\pm}G^{\pm}G^{\pm})$ and

DOI: 10.1021/acs.jpca.6b12296
J. Phys. Chem. A XXXX, XXX, XXX−XXX

$C_1(TG^{\pm}G^{\pm})$ conformers of TMP in the N_2 matrix.[22,23] It is clear from the figure that upon photolysis TMPhite is oxidized to TMP as new vibrational features characteristic of the P═O stretching region of TMP are produced. The photolysis experiments of TMPhite in the presence of O_2 yielded features at 1305.9, 1301.7, 1295.5, 1290.5, 1286.7, 1283.9, and 1276.8 cm^{-1} at 12 K. The comparison of the vibrational features of pure TMP in the O_2-doped N_2 matrix disclosed that the features characteristic of both $C_3(G^{\pm}G^{\pm}G^{\pm})$ and $C_1(TG^{\pm}G^{\pm})$ conformers of TMP are produced in the matrix during the photooxidation of TMPhite. The strong, broad doublet feature at 1305.9/1301.7 cm^{-1} relative to the weak feature at 1286.7 cm^{-1} in the photooxidation experiments (Figure 3, grid B) clearly revealed the dominant presence of the $C_1(TG^{\pm}G^{\pm})$ conformer of TMP produced from the $C_1(TG^{\pm}G^{\pm})$ TMPhite precursor in preference to the $C_3(G^{\pm}G^{\pm}G^{\pm})$ conformer. Of course, there is a slight shift in the higher-wavenumber component of TMP produced through the photolytic route (1305.9 cm^{-1} is red shifted by 0.6 cm^{-1} with respect to 1306.5 cm^{-1} for pure TMP). It is also obvious from Figure 3 that the relative intensity of the $C_1(TG^{\pm}G^{\pm})$ conformer (1305.9/1301.7 cm^{-1}) with respect to the $C_3(G^{\pm}G^{\pm}G^{\pm})$ conformer (1283.9/1276.8 cm^{-1}) of TMP formed from photolysis is not identical to that of pure TMP.

In addition to the P═O spectral region, the P−O vibrational region is also considered to investigate the conformational composition of TMP as a result of the photooxidation of TMPhite. Figure 4 shows a comparison of photooxidized

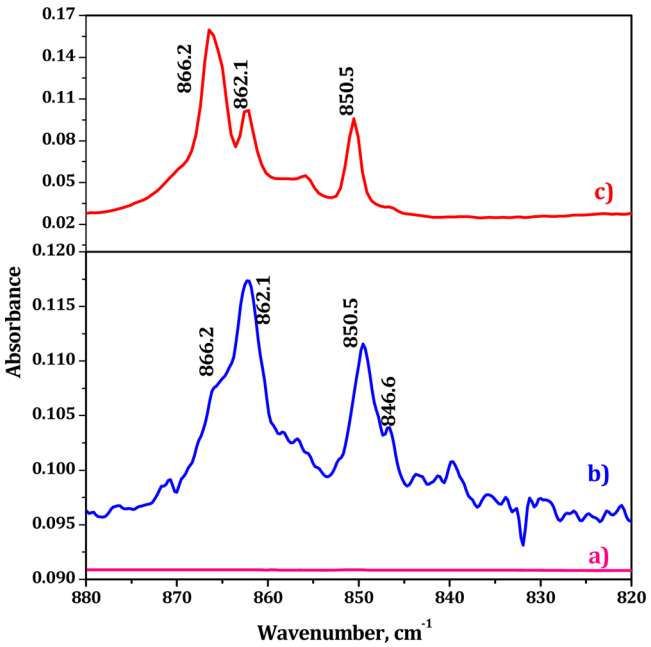

Figure 4. Infrared spectra of oxygen-doped TMPhite in the N_2 matrix in the P−O spectral region of TMP. (a) TMPhite/N_2 with 5% $^{16}O_2$ before photolysis at 12 K. (b) Same as in a but photolyzed for 30 min. (c) TMP/N_2 with 5% $^{16}O_2$ at 12 K.

TMPhite and pure TMP in the O_2-doped N_2 matrix in the P−O stretching region. The feature that occurs at 866.2 cm^{-1} was assigned to the $C_3(G^{\pm}G^{\pm}G^{\pm})$ conformer, whereas the other two features observed at 862.1 and 850.5 cm^{-1} were attributed to the $C_1(TG^{\pm}G^{\pm})$ conformer of TMP in the N_2 matrix.[22,23] It is therefore clear that the photooxidation produces features characteristic of the $C_1(TG^{\pm}G^{\pm})$ conformer at a higher intensity than for the $C_3(G^{\pm}G^{\pm}G^{\pm})$ conformer, which confirms the dominant production of the $C_1(TG^{\pm}G^{\pm})$ conformer compared to the C_3 $(G^{\pm}G^{\pm}G^{\pm})$ and is consistent with the observation made in the P═O stretching region. The C−O vibrational region of TMP, produced through photolysis, was broadened because the region occurs very close to the parent TMPhite absorption (Figure S1 in Supporting Information) and therefore is not considered in analyzing the conformational population.

In the photooxidation experiments, in addition to the generation of TMP in situ under matrix-isolated conditions, with small intensity, the spectral features of O_3[42,43] and N_2O[44] were also observed (not shown in the figure), which clearly suggest that oxygen atoms are indeed produced in the matrix during photolysis and that they react with O_2 and N_2 to form the aforementioned products. Of course, the generation of TMP from TMPhite itself confirms the production of oxygen atoms in the N_2 matrix. Therefore, to identify the source of oxygen atoms, blank experiments were carried out by photolyzing the O_2-doped N_2 matrix without TMPhite. This exercise produced neither O_3 nor N_2O in the N_2 matrix, probably indicating that TMPhite alone is the light-absorbing chromophore in the matrix. The nonformation of O_3 in the N_2 matrix is due to the ozone-free xenon arc lamp used in the photolysis experiments, which has negligible intensity in the 200−250 nm region (output 0.31%). It has been reported by Schriver-Mazzuoli et al. that O_3 is produced in the wavelength range of 245−266 nm.[45] The UV−visible absorption spectrum of pure TMPhite was recorded, and the maximum absorption was observed at 232 nm with tailing beyond 250 nm (Figure S5 in Supporting Information). The absorption beyond 250 nm could possibly be responsible for TMPhite behaving as a light-absorbing species in the photooxidation experiments.

The photooxidation experiments unambiguously revealed that the photochemical addition of oxygen to TMPhite does yield predominantly the higher-energy $C_1(TG^{\pm}G^{\pm})$ conformer. The population of the $C_1(TG^{\pm}G^{\pm})$ conformer of TMP thus produced via photooxidation is more than the as-deposited pure TMP in the O_2-doped N_2 matrix, and the nonequilibrium population is therefore achieved in the matrix.

Because TMPhite exists only in the ground-state $C_1(TG^{\pm}G^{\pm})$ conformer, one would expect to form the $C_1(TG^{\pm}G^{\pm})$ conformer of TMP exclusively in the photolysis experiment, and to our surprise, a small amount of the $C_3(G^{\pm}G^{\pm}G^{\pm})$ conformer of TMP was also observed. The formation of the $C_3(G^{\pm}G^{\pm}G^{\pm})$ conformer of TMP could be due to the localized heating of the matrix during photoirradiation. During photolysis, the TMPhite molecule is electronically excited through photon absorption, and the excess energy gets dissipated to the surrounding matrix, which causes the localized heating of the matrix. As a result, the $C_3(G^{\pm}G^{\pm}G^{\pm})$ conformer is produced at the expense of the freshly formed $C_1(TG^{\pm}G^{\pm})$ conformer of TMP from TMPhite. Because the $C_3(G^{\pm}G^{\pm}G^{\pm})$ conformer of TMP is energetically favorable in the potential energy surface, the route by which it is formed at low temperatures is through the energy dissipation in the matrix from the higher-energy $C_1(TG^{\pm}G^{\pm})$ conformer. Furthermore, the operation of the nonequilibration of excited rotamers (NEER) principle needs to be considered in the photoprocess.[46,47] As a direct consequence of NEER, the photooxidation of TMPhite is expected to produce TMP, which is predominately enriched in the $C_1(TG^{\pm}G^{\pm})$ conformation. The fact that a small amount of the $C_3(G^{\pm}G^{\pm}G^{\pm})$ conformer of TMP is also produced in addition to the $C_1(TG^{\pm}G^{\pm})$ conformer should be due to conformational cooling

DOI: 10.1021/acs.jpca.6b12296
J. Phys. Chem. A XXXX, XXX, XXX−XXX

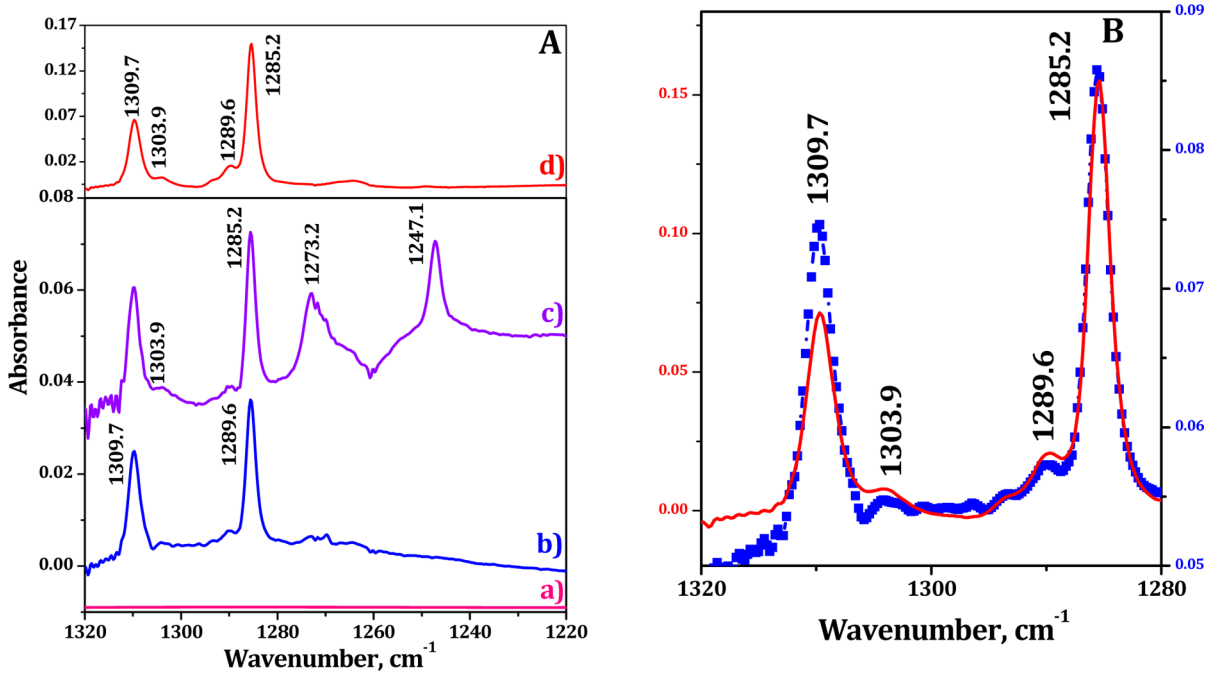

Figure 5. Comparison of photoirradiation experiments of oxygen-doped TMPhite in *p*-H_2 (grid A) and conformational yield comparison (grid B) in the P═O spectral region of TMP. Grid A: Infrared spectra of (a) TMPhite/*p*-H_2 with 5% $^{16}O_2$ before photolysis at 2.5 K. (b) Same as in a but photolyzed for 30 min. (c) TMPhite/*p*-H_2 with 2.5% $^{16}O_2$ and 2.5% $^{18}O_2$ after photolysis at 2.5 K. (d) TMP/*p*-H_2 with 5% $^{16}O_2$ at 2.5 K. Grid B: Blue-[line + symbol], infrared spectra of TMP produced through the photooxidation of TMPhite in the *p*-H_2 matrix; red-[line], pure TMP/*p*-H_2 with 5% $^{16}O_2$ at 2.5 K. The typical concentration of TMPhite or TMP to matrix is 1:1000.

that is occurring to a smaller extent by the light-induced local heating of the matrix surrounding the molecule, which causes the rigid matrix to become soft.

Clearly, the $C_3(G^{\pm}G^{\pm}G^{\pm})$ conformer of TMPhite is not responsible for the production of the $C_3(G^{\pm}G^{\pm}G^{\pm})$ conformer of TMP, and a conformer of this symmetry of TMPhite is the highest-energy conformer in the energy ladder and has an insignificant population in the matrix. It is evident from Figure 3 (grid A, trace c) that the vibrational features corresponding to isotopic scrambling experiments (with mixtures of $^{16}O_2$ and $^{18}O_2$) produced additional features that are red-shifted by ∼35 cm^{-1}, which correspond to the P═^{18}O stretching of TMP generated via photoirradiation. The experimental P═^{18}O shift with respect to P═^{16}O stretching matches well with the computed shift (at the B3LYP/6-311++G(d,p) level of theory) for $C_3(G^{\pm}G^{\pm}G^{\pm})$ and $C_1(TG^{\pm}G^{\pm})$ conformers of TMP respectively (Table 2). For TMP with ^{18}O, in the P═O region, the experimental shift for the $C_3(G^{\pm}G^{\pm}G^{\pm})$ conformer was 38.7 cm^{-1} whereas the shift was 38.9 and 39.3 cm^{-1} for the $C_1(TG^{\pm}G^{\pm})$ conformer in the N_2 matrix with respect to TMP with ^{16}O.

The results of photooxidation experiments performed in the pure O_2 matrix are similar to what was observed in the case of the N_2 matrix. As a corollary to the N_2 matrix, multiple features were observed in the P═O stretching region of TMP in the O_2 matrix. The infrared spectra of photoirradiation experiments performed in the O_2 matrix are shown in Figure S2 of the Supporting Information. Notably, in the O_2 matrix, the TMPhite precursor was completely converted to TMP during photolysis, unlike in the N_2 matrix. It has been roughly estimated that in the N_2 matrix ∼20% of initially deposited TMPhite is converted to TMP. In addition to the P═O stretching region, in the Supporting Information (Figure S1 and S2) the results of photoirradiation experiments in pure O_2 and O_2-doped N_2 matrixes in the O−C and P−O stretching regions are presented and the product features of TMP are appropriately marked. To show the partial oxidation of TMPhite in the O_2-doped N_2 matrix and complete oxidation in the pure O_2 matrix, in Figure S3 of the Supporting Information the results of photolysis in the complete spectral region are overlapped.

It is apparent that the infrared spectra obtained from the photooxidation experiment of TMPhite varies compared to the spectra of pure TMP because the photolysis of TMPhite in the O_2-doped N_2 matrix yielded additional features in the P═O stretching region at 1295.5, 1290.5, 1283.9, and 1276.8 cm^{-1} and in the pure O_2 matrix at 1229.2, 1292.7, and 1274.8 cm^{-1}, which makes the spectral region congested and complicates the assignments. These additional features are not due to either TMP or TMPhite, hence they could probably be due to the some other photoproducts/adducts generated in the matrix. To check for such a possibility, additional experiments were conducted in the N_2 matrix to examine whether the products observed were due to the secondary products of TMP with oxygen as a result of photoirradiation and/or due to the adducts of either TMP/TMPhite and N_2O and/or adducts of TMP/TMPhite and O_3 in an N_2 matrix. These specific experiments did not produce the characteristic set of additional features observed during the photooxidation of TMPhite, and hence the assignments of these features to the above-mentioned products can safely be ruled out. Similarly, TMPhite can be expected to yield the photo-Arbuzov product, dimethyl methyl phosphonate (DMMP), a reaction that does not require oxygen because phosphites in solution when exposed to UV irradiation were reported to undergo photo-Arbuzov rearrangement.[48] Prolonged irradiation of TMPhite in an N_2 matrix (in the absence of an oxygen dopant) did not produce any characteristic vibrational features that could be assigned to DMMP, which further confirms that these spectral features are not due to the product of the photo-Arbuzov

DOI: 10.1021/acs.jpca.6b12296
J. Phys. Chem. A XXXX, XXX, XXX−XXX

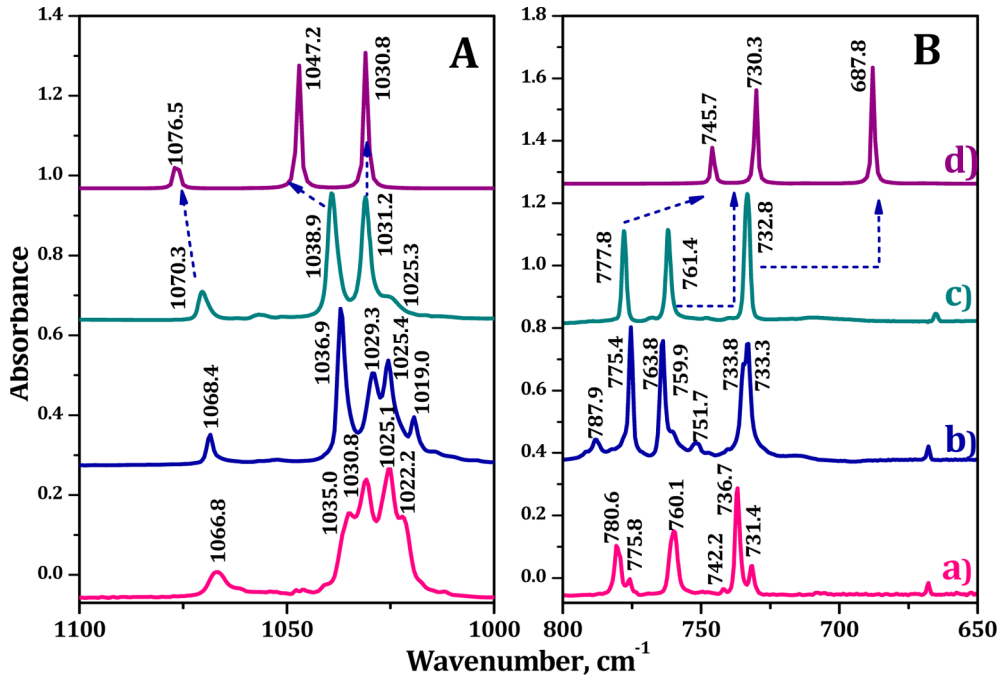

Figure 6. Comparison of infrared spectra of TMPhite in (a) N_2, (b) O_2, and (c) *p*-H_2 matrixes. (d) Calculated vibrational features of the ground-state $C_1(TG^{\pm}G^{\pm})$ conformer of TMPhite is shown for comparison. Grids A and B correspond to O−C and P−O stretching regions of TMPhite, respectively. The typical concentration of TMPhite to the matrix is 1:1000.

reaction. Probably, the matrix cage prevents the photo-Arbuzov rearrangement of TMPhite to produce DMMP.

If these additional features are not due to adducts or any other ancillary products, then subsequent probing is imperative to sort out to which group these features actually belong. To address this issue, experiments were performed in the *p*-H_2 matrix. Among the matrixes explored so far, the *p*-H_2 matrix host is inherently superior because of its condensed-phase properties, which provide a minimally perturbing environment for the guest molecule with a reduced or diminished cage effect. Therefore, photooxidation experiments were conducted in the *p*-H_2 matrix to envisage what difference *p*-H_2 actually makes in comparison to the conventional N_2 and O_2 matrixes.

3.2. Photooxidation of TMPhite in the *p*-H_2 Matrix. At the outset, the *p*-H_2 produced was examined for its purity by low-temperature infrared measurements.[40] When *p*-H_2 was directly deposited upon its production from the *p*-H_2 generator, the purity was estimated to be ∼99.3% (∼0.7% *o*-H_2). For experiments with TMPhite/TMP with *p*-H_2 gas, the *o*-H_2 concentration was found to be ∼1.5%. When experiments were performed with a 5% O_2 dopant, the paramagnetic O_2 increased the concentration of the *o*-H_2 impurity to ∼7%. In essence, the photooxidation experiments could be performed only with a *p*-H_2 purity of ∼93%. However, it was observed that at this higher level of *o*-H_2 impurity, additional splitting of the spectral features of both TMPhite and TMP was not observed.

When photoirradiation was performed under identical conditions on TMPhite with 5% $^{16}O_2$ in a *p*-H_2 matrix at 2.5 K, surprisingly, vibrational features in the P═^{16}O stretching region of TMP were obtained without any spectral congestion (Figure 5, grid A, traces b and d). The experiments performed using 2.5% $^{16}O_2$ and 2.5% $^{18}O_2$ in the *p*-H_2 matrix produced vibrational features characteristic of an isotopic shift corresponding to the P═^{18}O stretching region of TMP (Figure 5, grid A, trace c). The $C_3(G^{\pm}G^{\pm}G^{\pm})$ and $C_1(TG^{\pm}G^{\pm})$ conformers of TMP exhibited isotopic (^{18}O) shifts of 38.1 and 36.5 cm^{-1} with respect to ^{16}O, respectively, in the *p*-H_2 matrix.

In other words, the secondary features, those obtained in the N_2 and O_2 matrixes, were not observed in the *p*-H_2 matrix. Furthermore, the spectrum of TMP produced through the photolytic route is very simple in contrast to those of the N_2 and O_2 matrixes. Therefore, the photooxidation experiments performed in the *p*-H_2 matrix clearly delineate that the product is only TMP and no other secondary products are formed. It is important to point out that the vibrational features of TMP in the 5% O_2-doped *p*-H_2 matrix exhibited a slight blue shift of 2 cm^{-1} with respect to pure TMP in the *p*-H_2 matrix. In the Supporting Information (Figure S4), the results of photoirradiation experiments in the O_2-doped *p*-H_2 matrix in the O−C and P−O stretching regions are presented.

To rationalize the experimental observation in the *p*-H_2 matrix, the infrared spectra of TMPhite, the photoprecursor, was critically examined. It is clear from the O−C (Figure 6, grid A) and P−O (Figure 6, grid B) stretching regions of TMPhite that the infrared spectrum in the *p*-H_2 matrix is free from multiple site effects, unlike in the N_2 and O_2 matrixes. The computed spectrum of the $C_1(TG^{\pm}G^{\pm})$ conformer of TMPhite (Figure 6, trace d) is given for comparison. It can be recalled that for TMPhite the ground-state $C_1(TG^{\pm}G^{\pm})$ conformer alone is populated in low-temperature matrixes. Clearly the simple spectrum, free from site effects, is attributable to the quantum crystal nature of *p*-H_2, and conventional N_2 and O_2 matrixes suffer severely because of the site effect. Because of the tight cage effect of the N_2 and O_2 matrixes, these site-split features of TMPhite are retained after its photooxidation to TMP and are manifested as additional features in the experiment. Certainly, the cage surrounding the TMP produced from TMPhite photooxidation is not identical to the cage formed when pure TMP vapor was immediately deposited onto the matrix. It is expected that annealing can transform all different site-split

DOI: 10.1021/acs.jpca.6b12296
J. Phys. Chem. A XXXX, XXX, XXX−XXX

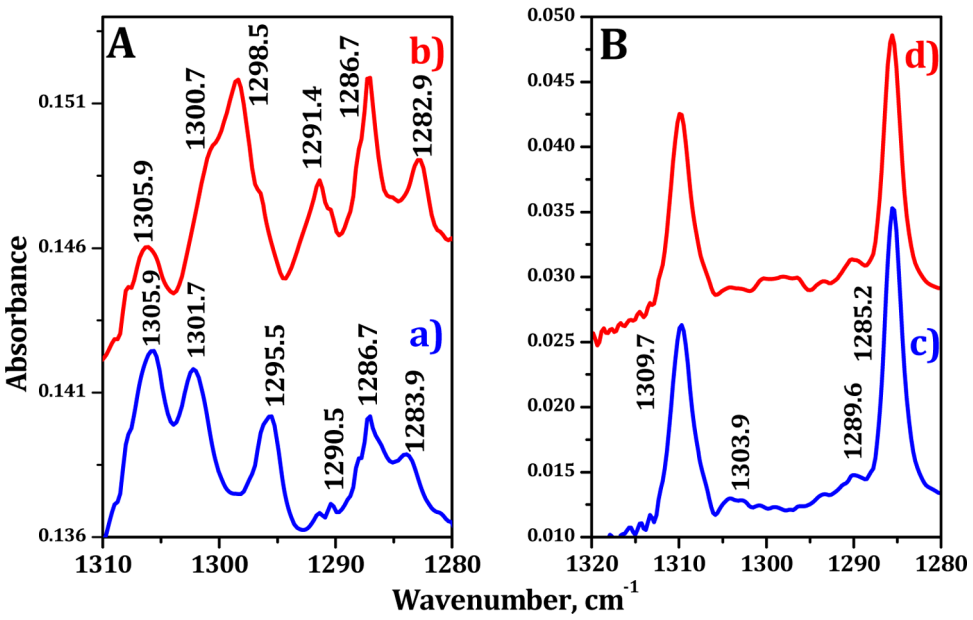

Figure 7. Effect of annealing on the photolyzed sample of 5% O_2-doped TMPhite. Grid A (N_2 matrix): (a) as deposited and photoirradiated at 12 K and (b) the annealed sample at 30 K after photoirradiation. Grid B (p-H_2 matrix): (c) as deposited and photoirradiated at 2.5 K and (d) the annealed sample at 4.5 K after photoirradiation.

features irreversibly to the stable ones, but surprisingly, on the annealing of the N_2 matrix, the features at 1301.7 and 1295.5 cm^{-1} widened and merged to form a broad feature centered at 1298.5 cm^{-1} in comparison to the photooxidized sample (Figure 7, grid A, trace b). In addition, the weak shoulders observed at 1290.5/1283.9 cm^{-1} are shifted to 1291.4/1282.9 cm^{-1} with the increase in intensity on annealing. This observation implies that the cage effect is still operative under the conditions of annealing, whereas in the p-H_2 matrix the annealing to the highest possible temperature of 4.5 K does not change the intensity of the features produced through photooxidation (Figure 7, grid B). Another striking difference between the conventional N_2 and O_2 matrixes and the p-H_2 matrix is the composition of $C_3(G^{\pm}G^{\pm}G^{\pm})$ and $C_1(TG^{\pm}G^{\pm})$ conformers of TMP formed. Whereas $C_1(TG^{\pm}G^{\pm})$-rich TMP was produced in N_2 and O_2 matrixes, the proportion of the $C_1(TG^{\pm}G^{\pm})$ conformer is much less in the p-H_2 matrix, and the near-equilibrium population was achieved in comparison to pure TMP in the p-H_2 matrix (Figure 5, grid B). The intrinsically restless nature of the p-H_2 molecule with a large-amplitude zero-point vibration and a large lattice constant is likely responsible for achieving the near-equilibrium population.

4. CONCLUSIONS

In this work, the photooxidation of TMPhite in N_2, O_2, and p-H_2 matrixes was studied. When TMP was produced in situ in low-temperature matrixes through the photolytic pathway, the nascent population distribution of $C_3(G^{\pm}G^{\pm}G^{\pm})$ and $C_1(TG^{\pm}G^{\pm})$ conformers was considerably affected. In comparison to the conformational composition of pure TMP, photooxidation produced a preponderantly enriched $C_1(TG^{\pm}G^{\pm})$ conformer in the presence of a little $C_3(G^{\pm}G^{\pm}G^{\pm})$ conformer of TMP, thereby producing a nonequilibrium conformational distribution at low temperatures. The presence of the ground-state $C_1(TG^{\pm}G^{\pm})$ conformation of TMPhite, the photolytic precursor, was attributed to the enrichment of the $C_1(TG^{\pm}G^{\pm})$ conformer of TMP.

Nevertheless, both TMPhite and TMP are expected to be structurally alike with the similar conformational landscape except for the presence of extra oxygen in TMP, the unique stereoelectronic factors were observed to alter the individual conformational preferences. The presence of phosphoryl group has a profound influence on the conformational control of TMP and in turn, the geminal hyperconjugative charge-transfer delocalization interactions regulate the conformational space of both TMPhite and TMP.

Another significant outcome of this study is the interesting variation in photolytic behavior observed in the case of p-H_2. In the conventional N_2 and O_2 matrixes, multiple spectral features during the photooxidation of TMPhite were observed. The multiple features on photooxidation are simply the manifestations of site-splitting of the ground-state $C_1(TG^{\pm}G^{\pm})$ conformer of TMPhite. The site splitting of the photoproduct was observed to be preserved on annealing because of the cage effect of N_2 and O_2 matrixes. Consequently, this work highlights that among the matrixes, p-H_2 is superior as site effects on either the precursor or the photoproduct were found to be automatically repaired as a result of its quantum crystal nature. Furthermore, in the p-H_2 matrix, the near-equilibrium or equilibrium conformational population was achieved because TMP/TMPhite molecules embedded in the p-H_2 matrix can be considered to be conformationally labile.

■ ASSOCIATED CONTENT

Supporting Information

The Supporting Information is available free of charge on the ACS Publications website at DOI: 10.1021/acs.jpca.6b12296.

Dihedral angles of TMP and TMPhite. Infrared spectra of matrix-isolated TMPhite with an oxygen-doped N_2 matrix in the O−C and P−O stretching regions, of O_2-doped TMPhite before and after photolysis in the P═O, O−C, and P−O stretching regions in N_2 and O_2 matrixes, of matrix-isolated TMPhite in the oxygen matrix, and of oxygen-doped TMPhite in the p-H_2 matrix in the O−C

DOI: 10.1021/acs.jpca.6b12296
J. Phys. Chem. A XXXX, XXX, XXX−XXX

and P−O stretching regions. UV−visible absorption spectrum of pure TMPhite. (PDF)

AUTHOR INFORMATION

Corresponding Author

*E-mail: sundar@igcar.gov.in.

ORCID

K. Sundararajan: 0000-0002-9961-0030

Notes

The authors declare no competing financial interest.

ACKNOWLEDGMENTS

The authors thank Prof. D. Mohan, Department of Chemical Engineering, A. C. Tech Campus, Anna University, Chennai, India, for providing computational support. R.G. gratefully acknowledges the grant of a research fellowship from IGCAR, Department of Atomic Energy, India. The authors thank the anonymous reviewers for critically and meticulously analyzing this work, which resulted in the constructive improvement of the article.

REFERENCES

(1) Westheimer, F. H. Why Nature Chose Phosphates. *Science* **1987**, *235*, 1173−1178.

(2) Hirsch, A. K. H.; Fischer, F. R.; Diederich, F. Phosphate Recognition in Structural Biology. *Angew. Chem., Int. Ed.* **2007**, *46*, 338−352.

(3) Badenhoop, J. K.; Weinhold, F. Natural Bond Orbital Analysis of Steric Interactions. *J. Chem. Phys.* **1997**, *107*, 5406−5421.

(4) Goodman, L.; Pophristic, V.; Weinhold, F. Origin of Methyl Internal Rotation Barriers. *Acc. Chem. Res.* **1999**, *32*, 983−993.

(5) Pophristic, V.; Goodman, L. Hyperconjugation Not Steric Repulsion Leads to the Staggered Structure of Ethane. *Nature* **2001**, *411*, 565−568.

(6) Mo, Y.; Gao, J. Theoretical Analysis of the Rotational Barrier of Ethane. *Acc. Chem. Res.* **2007**, *40*, 113−119.

(7) Lemieux, R. U.; Kullnig, R. K.; Bernstein, H. J.; Schneider, W. G. Configurational Effects on the Proton Magnetic Resonance Spectra of Six-membered Ring Compounds. *J. Am. Chem. Soc.* **1958**, *80*, 6098−6105.

(8) Bailey, W. F.; Eliel, E. L. Conformational analysis. XXIX. 2-Substituted and 2,2-Disubstituted 1,3-dioxanes. Generalized and Reverse Anomeric Effects. *J. Am. Chem. Soc.* **1974**, *96*, 1798−1806.

(9) Norskov-Lauritsen, L.; Allinger, N. L. A Molecular Mechanics Treatment of the Anomeric Effect. *J. Comput. Chem.* **1984**, *5*, 326−335.

(10) Perron, F.; Albizati, K. F. Chemistry of Spiroketals. *Chem. Rev.* **1989**, *89*, 1617−1661.

(11) Dubois, J. E.; Cossé-Barbia, A.; Watson, G. D. When Local Crowding Reinforces an Anomeric Effect. *Tetrahedron Lett.* **1989**, *30*, 167−170.

(12) Senderowitz, H.; Golender, L.; Fuchs, B. New Supramolecular Host Systems. 2. 1,3,5,7-Tetraoxadecalin, 1,2-Dimethoxyethane and the Gauche Effect Reappraised. Theory *vs.* Experiment. *Tetrahedron* **1994**, *50*, 9707−9728.

(13) Venkatesan, V.; Sundararajan, K.; Sankaran, K.; Viswanathan, K. S. Conformations of Dimethoxymethane: Matrix Isolation Infrared and ab Initio Studies. *Spectrochim. Acta, Part A* **2002**, *58*, 467−478.

(14) Weinhold, F.; Landis, C. *Valency and Bonding: A Natural Bond Orbital Donor-Acceptor Perspective*; Cambridge University Press: Cambridge, U.K., 2005.

(15) Ramanathan, N. Ph.D. Thesis. University of Madras, 2013.

(16) Sood, D. D.; Patil, S. K. Chemistry of Nuclear Fuel Reprocessing: Current status. *J. Radioanal. Nucl. Chem.* **1996**, *203*, 547−573.

(17) Ramanathan, N.; Sundararajan, K.; Kar, B. P.; Viswanathan, K. S. Conformations of Trimethyl Phosphite: A Matrix Isolation Infrared and ab Initio Study. *J. Phys. Chem. A* **2011**, *115*, 10059−10068.

(18) The reason for keeping the phosphorus lone pair as a reference in TMPhite is to have a common conformational terminology for both TMPhite and TMP because the conformations are named by fixing the phosphoryl group as a reference in TMP. Because the positions of the lone pair in TMPhite and the phosphoryl group in TMP are identical, the lone pair in TMPhite is taken as a reference. Furthermore, if a lone pair is taken as a reference, then there will be commonality in the conformations of TMPhite and TMP.

(19) Borba, A.; Zavaglia, A. G.; Simoes, P. N. N. L.; Fausto, R. Matrix Isolation FTIR Spectroscopic and Theoretical Study of Dimethyl Sulfite. *J. Phys. Chem. A* **2005**, *109*, 3578−3586.

(20) Borba, A.; Gomez-Zavaglia, A.; Fausto, R. Conformational Cooling and Conformation Selective Aggregation in Dimethyl Sulfite Isolated in Solid Rare Gases. *J. Mol. Struct.* **2006**, *794*, 196−203.

(21) Reva, I. D.; Ilieva, S. V.; Fausto, R. Conformational Isomerism in Methyl Cyanoacetate: A Combined Matrix-Isolation Infrared Spectroscopy and Molecular Orbital Study. *Phys. Chem. Chem. Phys.* **2001**, *3*, 4235−4241.

(22) Vidya, V.; Sankaran, K.; Viswanathan, K. S. Matrix Isolation-Supersonic Jet Infrared Spectroscopy: Conformational Cooling in Trimethyl Phosphate. *Chem. Phys. Lett.* **1996**, *258*, 113−117.

(23) George, L.; Viswanathan, K. S.; Singh, S. Ab Initio Study of Trimethyl Phosphate: Conformational Analysis, Dipole Moments, Vibrational Frequencies, and Barriers for Conformer Interconversion. *J. Phys. Chem. A* **1997**, *101*, 2459−2464.

(24) Reva, I.; Simao, A.; Fausto, R. Conformational Properties of Trimethylphosphate Monomer. *Chem. Phys. Lett.* **2005**, *406*, 126−136.

(25) Reva, I.; Lapinski, L.; Nowak, M. J. Photoinduced Oxidation of Triphenylphosphine Isolated in a Low-temperature Oxygen Matrix. *Chem. Phys. Lett.* **2008**, *467*, 97−100.

(26) Gush, H. P.; Har, W. F. J.; Allin, E. J.; Welsh, H. L. The Infrared Fundamental Band of Liquid and Solid Hydrogen. *Can. J. Phys.* **1960**, *38*, 176−193.

(27) Crane, A.; Gush, H. P. The Induced Infrared Absorption of Solid Deuterium and Solid Hydrogen Deuteride. *Can. J. Phys.* **1966**, *44*, 373−398.

(28) Silvera, I. F. The Solid Molecular Hydrogens in the Condensed Phase: Fundamentals and Static Properties. *Rev. Mod. Phys.* **1980**, *52*, 393−452.

(29) Kranendonk, J. V. *Solid Hydrogen*; Plenum: New York, 1982.

(30) Oka, T. High Resolution Spectroscopy of Solid Hydrogen. *Annu. Rev. Phys. Chem.* **1993**, *44*, 299−333.

(31) Momose, T.; Miki, M.; Uchida, M.; Shimizu, T.; Yoshizawa, I.; Shida, T. Infrared Spectroscopic Studies on Photolysis of Methyl Iodide and its Clusters in Solid Parahydrogen. *J. Chem. Phys.* **1995**, *103*, 1400.

(32) Momose, T.; Miki, M.; Wakabayashi, T.; Shida, T.; Chan, M. C.; Lee, S.; Oka, T. Infrared Spectroscopic Study of Rovibrational States of Methane Trapped in Parahydrogen Crystal. *J. Chem. Phys.* **1997**, *107*, 7707.

(33) Mengel, M.; Winnewisser, B. P.; Winnewisser, M. New Infrared Transitions in Solid Parahydrogen in the MIR and NIR/VIS Regions. *J. Mol. Spectrosc.* **1998**, *188*, 221−244.

(34) Tam, S.; Fajardo, M. E. Ortho/Para Hydrogen Converter for Rapid Deposition Matrix Isolation Spectroscopy. *Rev. Sci. Instrum.* **1999**, *70*, 1926−1932.

(35) Fajardo, M. E. In *Solid Para Hydrogen a Primer in Physics and Chemistry at Low Temperatures*; Khriachtchev, L., Ed.; Pan Stanford: Singapore, 2011; Chapter 6.

(36) Sogoshi, N.; Wakabayashi, T.; Momose, T.; Shida, T. Infrared Spectroscopic Studies on Photolysis of Ethyl Iodide in Solid Parahydrogen. *J. Phys. Chem. A* **1997**, *101*, 522−527.

(37) Huang, C.-W.; Lee, Y. C.; Lee, Y.-P. Diminished Cage Effect in Solid p-H_2: Infrared Spectra of ClSCS, ClCS, and ClSC in an Irradiated p-H_2 Matrix Containing Cl_2 and CS_2. *J. Chem. Phys.* **2010**, *132*, 164303.

(38) Bahou, M.; Lee, Y.-P. Diminished Cage Effect in Solid p-H_2: Infrared Absorption of CH_3S Observed from Photolysis *in situ* of CH_3SH, CH_3SCH_3, or CH_3SSCH_3 Isolated in p-H_2 Matrices. *J. Chem. Phys.* **2010**, *133*, 164316.

DOI: 10.1021/acs.jpca.6b12296
J. Phys. Chem. A XXXX, XXX, XXX−XXX

(39) Bahou, M.; Das, P.; Lee, Y.-F.; Wub, Y.-P.; Lee, Y.-P. Infrared Spectra of Free Radicals and Protonated Species Produced in Para-Hydrogen Matrices. *Phys. Chem. Chem. Phys.* **2014**, *16*, 2200−2210.
(40) Sundararajan, K.; Sankaran, K.; Ramanathan, N.; Gopi, R. Production and Characterization of Para-Hydrogen Gas for Matrix Isolation Infrared Spectroscopy. *J. Mol. Struct.* **2016**, *1117*, 181−191.
(41) Frisch, M. J.; Trucks, G. W.; Schlegel, H. B.; Scuseria, G. E.; Robb, M. A.; Cheeseman, J. R.; Scalmani, G.; Barone, V.; Mennucci, B.; Peterson, G. A.; et al. *Gaussian 09*, Revision D.01; Gaussian Inc.: Wallingford, CT, 2009.
(42) Schriver-Mazzuoli, L.; Schriver, A.; Lugez, C.; Perrin, A.; Peyret, C. C.; Flaud, J.-M. Vibrational Spectra of the $^{16}O/^{17}O/^{18}O$ Substituted Ozone Molecule Isolated in Matrices. *J. Mol. Spectrosc.* **1996**, *176*, 85−94.
(43) Sundararajan, K.; Sankaran, K.; Kavitha, V. Reactions of Laser-Ablated Tellurium Atoms with Oxygen Molecules: Matrix Isolation Infrared and DFT Studies. *J. Mol. Struct.* **2008**, *876*, 240−249.
(44) Bahou, M.; Schriver-Mazzuoli, L.; Peyret, C. C.; Schriver, A.; Chiavassa, T.; Aycard, J. P. Infrared Matrix Spectra of the $N_2O\cdots O_2$ Complex in Solid Nitrogen. The $N_2O\cdots O_2$ + O Thermal Diffusion Limited Reaction. *Chem. Phys. Lett.* **1997**, *265*, 145−153.
(45) Schriver-Mazzuoli, L.; Saxce, A.; De Lugez, C.; Peyret, C. C.; Schriver, A. Ozone Generation through Photolysis of an Oxygen Matrix at 11 K: Fourier Transform Infrared Spectroscopy Identification of the $O\cdots O_3$ Complex and Isotopic Studies. *J. Chem. Phys.* **1995**, *102*, 690−701.
(46) Bernardi, F.; Olivucci, M.; Robb, M. A. Following Reaction Paths in Organic Photochemistry: The Special Role of Surface Crossings. *Pure Appl. Chem.* **1995**, *67*, 17−24.
(47) Brouwer, A. M.; Jacobs, H. J. C. Photochemistry of 2,5-Dimethyl-1,3,5-Hexatrienes in Argon Matrices. Formation of Isomers and Rotamers. *Recl. Trav. Chim. Pays-Bas.* **1995**, *114*, 449−458.
(48) Bhanthumnavin, W.; Bentrude, W. G. Photo-Arbuzov Rearrangements of 1-Arylethyl Phosphites: Stereochemical Studies and the Question of Radical-Pair Intermediates. *J. Org. Chem.* **2001**, *66*, 980−990.

DOI: 10.1021/acs.jpca.6b12296
J. Phys. Chem. A XXXX, XXX, XXX−XXX